RAA 2017 Vol. **17** No. **2**, 15 (6pp) doi: 10.1088/1674–4527/17/2/15

http://www.raa-journal.org *http://iopscience.iop.org/raa*

***R**esearch in*
***A**stronomy and*
***A**strophysics*

Double-lined M dwarf eclipsing binaries from Catalina Sky Survey and LAMOST

Chien-Hsiu Lee[1] and Chien-Cheng Lin[2]

[1] Subaru Telescope, National Astronomical Observatory of Japan, 650 North Aohoku Place, Hilo, HI 96720, USA; *leech@naoj.org*

[2] Shanghai Astronomical Observatory, Chinese Academy of Sciences, Shanghai 200030, China; *cclin@shao.ac.cn*

Received 2016 August 25; accepted 2016 October 20

Abstract Eclipsing binaries provide a unique opportunity to determine fundamental stellar properties. In the era of wide-field cameras and all-sky imaging surveys, thousands of eclipsing binaries have been reported through light curve classification, yet their basic properties remain unexplored due to the extensive efforts needed to follow them up spectroscopically. In this paper we investigate three M2-M3 type double-lined eclipsing binaries discovered by cross-matching eclipsing binaries from the Catalina Sky Survey with spectroscopically classified M dwarfs from the Large Sky Area Multi-Object Fiber Spectroscopic Telescope survey data release one and two. Because these three M dwarf binaries are faint, we further acquire radial velocity measurements using GMOS on the Gemini North telescope with R ∼4000, enabling us to determine the mass and radius of individual stellar components. By jointly fitting the light and radial velocity curves of these systems, we derive the mass and radius of the primary and secondary components of these three systems, in the range between 0.28–0.42 $M_{\odot}$ and 0.29–0.67 $R_{\odot}$, respectively. Future observations with a high resolution spectrograph will help us pin down the uncertainties in their stellar parameters, and render these systems benchmarks to study M dwarfs, providing inputs to improving stellar models in the low mass regime, or establishing an empirical mass-radius relation for M dwarf stars.

Key words: (stars:) binaries: eclipsing

1 INTRODUCTION

M dwarfs are located in the cool, low mass end of the main sequence; they are the most abundant stars in the Milky Way and are ubiquitous in the solar neighborhood. However, they are very faint in optical bands, and hence are difficult to discover and characterize. Thanks to advances in large spectroscopic surveys using medium-class telescopes equipped with wide-field cameras and multi-object spectrographs, such as the Sloan Digital Sky Survey (York et al. 2000) and Large Sky Area Multi-Object Fiber Spectroscopic Telescope (LAMOST, Cui et al. 2012), hundreds of thousands of M dwarfs have been spectroscopically confirmed to date (West et al. 2011; Guo et al. 2015).

Recent progress in spectroscopic studies of M dwarfs also presents challenges for theoretical modeling. For example, it has been found that there are discrepancies between theoretical modeling and observations of M dwarfs. The models often underpredict the size and overpredict the temperature of M dwarfs (see e.g. Zhou et al. 2015), especially in the very low mass end ($M < 0.3\,M_{\odot}$) where the stars become completely convective and therefore difficult to model. Furthermore, it has been reported that M dwarfs exhibit strong magnetic activities, which might be linked to their inflated size. Deriving fundamental parameters of M dwarfs has drawn more and more interest, especially because an increasing number of exoplanets discovered by the *Kepler* mission are hosted by M-type stars (Dressing & Charbonneau 2013). For transiting exoplanets, precise and accurate measurements of the host star parameters are crucial for deriving an exoplanet's radius, which is essential for inferring the density of the exoplanet and determining if it is a gaseous, Jupiter-like planet or a rocky planet like Earth. In this regard, improving

theoretical modeling of M dwarf stars, or establishing an empirical mass-radius relation for M dwarfs, is highly desired.

Eclipsing binaries provide us with unique opportunities to directly measure the mass, radius and effective temperature of individual stars down to the level of a few percent. Their light curves can provide information on the inclination angle, orbital period, eccentricity, mass ratio and radius in terms of the semi-major axis. On the other hand, spectroscopic observations can enable us to derive the mass and effective temperature of individual stars, as well as their orbital distance. The degeneracy in normal effective temperature and surface gravity that is associated with extracting information from a single star spectrum is not an issue for eclipsing binaries. This is because we can directly determine the mass and radius to derive the surface gravity independently, hence breaking the degeneracy and unambiguously determining the temperature of the binaries.

This work reports the discovery of three double-lined M dwarf eclipsing binary systems by analyzing data from both the Catalina Sky Survey (CSS) and the LAMOST survey, as well as dedicated spectroscopic follow-ups using the Gemini North telescope. This paper is organized as follows: in Section 2 we describe the photometric and spectroscopic observations at hand. We present our analysis in Section 3, followed by a discussion in Section 4 and prospects in Section 5.

2 DATA

2.1 Known M dwarfs from LAMOST

Because of their faintness in optical wavelengths, previous studies of M dwarfs were carried out using infrared imaging (see e.g. Lépine & Gaidos 2011; Thompson et al. 2013). Thanks to advances in wide-field cameras, multi-object spectrographs and all sky surveys with medium-sized telescopes, it is possible to obtain spectra to confirm M dwarfs in terms of quantity and quality. In this work we make use of the spectral catalog from LAMOST[1], a 4 m class telescope equipped with 4000 fibers distributed over a 5 degree field-of-view, with the capability of acquiring spectra from a wide range in the optical band (3700–9000 Å) with a resolution $R = 1800$ for targets as faint as $r = 19$ magnitude (Cui et al. 2012). Guo et al. (2015) have made use of LAMOST Data Release One (DR1), and present a sample of $\sim$ 93 000 spectroscopically confirmed and classified M dwarfs. In the recent LAMOST Data Release Two (DR2), there are $\sim$ 220 000 M dwarfs being cataloged, more than doubling the number of M dwarfs identified in LAMOST DR1. The LAMOST M dwarf sample was classified with the Hammer spectral typing facility (Covey et al. 2007), aided by visual inspection, ensuring that the spectral type is determined as precisely as within one subtype. This is by far the largest M dwarf sample confirmed spectroscopically to date, providing us with a firm basis to cross-match with eclipsing binaries found by other time-domain surveys.

2.2 Time Series Photometry from CSS

Since 2004, the CSS has constantly monitored the sky between –75<Dec<70 degrees using three small telescopes. To ensure coverage of most of the entire sky, two of the telescopes, i.e. the 0.7 m Catalina Schmidt Telescope (with an 8.2 deg^2 field of view (FOV)) and the 1.5 m Mount Lemmon Telescope (with a 1 deg^2 FOV) are in the northern hemisphere in Arizona, USA, while the 0.5 m Siding Spring Telescope (with a 4.2 deg^2 FOV) observes in the southern hemisphere, based in Australia. The main scientific driver of CSS is near Earth objects and potentially hazardous asteroids. Each telescope patrols its own patches of sky, excluding regions with Galactic latitude less than 15 degrees to avoid crowded stellar fields. The observations have been carried out without any filter to maximize throughput. These observations were taken in groups of four exposures separated by 10 minutes, with individual integration times as long as 30 seconds. After CCD reduction, the images were fed to SExtractor (Bertin & Arnouts 1996) for aperture photometry. Thanks to the high cadence and wide coverage, the survey is also valuable for time-domain science, enabling the Catalina Real-time Transient Survey (CRTS, Drake et al. 2009).

Data from the 0.7 m Catalina Schmidt Telescope between 2005 and 2011 were made public through Catalina Surveys Data Release[2]; the first data release (CSDR1) contains more than 200 million sources between 12 and 20 magnitude in V-band (Drake et al. 2013). Drake et al. (2014) searched for variables in CSDR1 in the region of –22<Dec<65 degrees, and identified $\sim$ 47 000 periodic variables using the Lomb-Scargle periodgram method. They further visually inspected the light curves and cataloged 4683 detached eclipsing binaries, the largest all-sky eclipsing binary catalog to date, providing a wealth of resources for time-series photometry.

[1] *http://www.lamost.org*

[2] *http://nesssi.cacr.caltech.edu/DataRelease/*

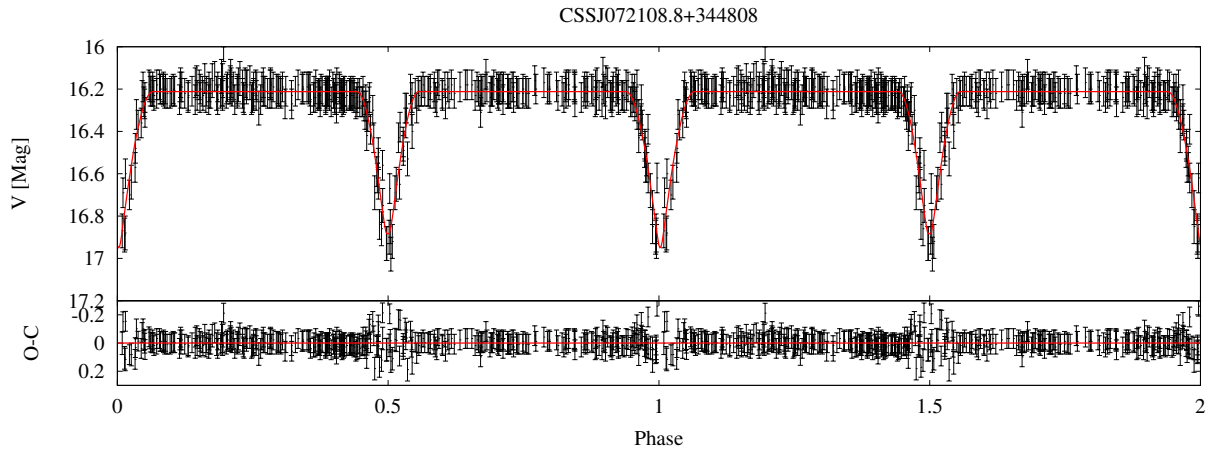

Fig. 1 Example CSS light curve of an M dwarf binary system. *Upper panel*: the CSS photometry is marked in *black*, while the best-fit DEBiL model (see Sect. 3) is marked in *red*. *Lower panel*: residuals of the best-fit DEBiL model.

3 ANALYSIS

3.1 Light Curve Analysis using DEBiL

As a starting point, we use the Detached Eclipsing Binary Light curve fitter[3] (DEBiL, Devor 2005) to analyze the light curves of our three M dwarf eclipsing binaries. DEBiL assumes a simple geometry to model the light curves: it forms an initial guess of the binary configuration from a set of analytic formulae for detached binaries (see e.g. Seager & Mallén-Ornelas 2003), and attempts to fit several parameters:

(1) The relative radius ($\frac{R_1}{a}$, $\frac{R_2}{a}$), in terms of the semi-major axis a.
(2) The brightness of both stars (mag_1, mag_2).
(3) The inclination angle (i), eccentricity (e) and argument of periastron (ω) of the binary orbit.

DEBiL fits the light curves in an iterative manner by minimizing χ^2 using the downhill simplex method (Nelder & Mead 1965) with simulated annealing (Press et al. 1992). Our best-fit results from DEBiL, as well as the light curve from CSDR1, are shown in Figure 1. The best-fit parameters from DEBiL are then fed to JKTEBOP for dynamical analysis in Section 3.3.

3.2 Radial Velocity Determination

As our eclipsing binaries are faint and their periods are short (P$\sim$0.4 – 1.3 days), to prevent smooth-out of the radial velocity (RV) curves, we need to reach a sufficient signal-to-noise ratio (S/N), i.e. S/N$>$50 within 0.1 period, which can be as short as one hour. In addition, a sufficient spectral resolution is also required to determine the masses and radii of the binary systems, preferably less than 1 Å pixel^{-1}. Only 8 m class telescopes are capable of reaching such high S/N and spectral resolution in the given amount of time. We thus conduct spectroscopic follow-up observations using the GMOS (Hook et al. 2004) on the Gemini North telescope via a fast turnaround program (Program ID GN-2016-FT16). We use the R831 grating with a 0.5 arcsecond slit, rendering a resolution of $R = 4396$, with the central wavelength at 7000 Å and a wavelength coverage of $\sim$2000 Å.

The observations were carried out on 2016 April 2 and 13 during the expected RV maxima at light curve quadrature (phase 0.25 and/or 0.75). In principle, we only need one observation at each quadrature to measure the RV maximum, nevertheless we aim to obtain two exposures per maximum, each with exposure times of 300 (CSSJ092128.3+332558), 400 (CSSJ074118.8+311434) and 600 (CSSJ072108.8+344808) seconds to reach high S/N. The second exposure can serve as a sanity check, ensuring we obtain consistent RV measurements at the same maximum. The GMOS data are reduced by using the dedicated IRAF[4] GMOS package[5] (v1.13) in a standard manner: each spectrum was bias subtracted, flat fielded, sky subtracted and wavelength calibrated using a CuAr lamp.

To extract RV information, we make use of the bright Hα emission line at 6562.8 Å. The Hα emissions from both stellar components are clearly resolved. We then fit the Hα line profile using a two-component

[3] *http://debil.droppages.com*

[4] *http://iraf.noao.edu*

[5] *http://www.gemini.edu/sciops/data-and-results/processing-software*

Table 1 RV Measurements from GMOS Observations

Epoch	$RV_1^\dagger$ [km s^{-1}]	$RV_2^\dagger$ [km s^{-1}]
CSSJ074118.8+311434		
57480.230475	202.05	22.86
57480.238484	203.42	23.77
57491.246632	56.68	195.19
CSSJ092128.3+332558		
57491.297419	138.51	–92.80
57491.301748	141.25	–90.05
57491.306088	143.99	–92.80
CSSJ072108.8+344808		
57480.359583	118.85	–128.45
57480.369097	117.48	–131.19

Notes: † The estimated error is $\pm$ 15 km s^{-1}.

Gaussian function. From the Gaussian fit, we obtain the radial velocity of each stellar component, as shown in Table 1, with an estimated error of 15 km s^{-1} based on the spectral resolution delivered by the R831 grating and 0.5 arcsecond slit (i.e. 3.4 Å pixel^{-1}).

3.3 Dynamical Analysis

With both the light curves and RV information in hand, we can determine the mass and radius of the system. We use JKTEBOP[6] (Southworth et al. 2004), a derivative of the EBOP code originally developed by Popper & Etzel (1981), with the capability of jointly fitting the light and RV curves to determine the mass and radius of each stellar component, as well as the parameters of the orbit. We fit the reference time of the primary eclipse (t_0), radius ratio of the primary to the secondary (R_2/R_1), radius sum in terms of semi-major axis ($\frac{R_1+R_2}{a}$), inclination angle (i), light ratio (L_2/L_1), orbital eccentricity (e), augment of periastron (ω), RV semi-amplitudes of the two components (K_1 and K_2) and systematic velocity ($V_{\rm sys}$). We use the best-fit results from DEBiL in Section 2.2 as an initial guess for most of the parameters; for semi-amplitudes K_1 and K_2, we assume the primary and secondary components have similar mass, and assume the RVs in Section 3.2 have approximately the maximum values, to estimate K_1 and K_2, respectively. The initial guess of the systematic velocity is taken as the mean of the estimated K_1 and K_2. The JKTEBOP fitting routine converges quickly (within 30 iterations), indicating the DEBiL results provide a good initial guess. Our best-fit JKTEBOP results are shown in Figure 2 (in red) and Table 2. We provide a detailed discussion of each eclipsing binary in the following section.

[6] *http://www.astro.keele.ac.uk/jkt/codes/jktebop.html*

Table 2 Best-fit Parameters for Our Eclipsing Binary Systems

Parameter	CSSJ0741	CSSJ0921	CSSJ0721
	System parameters		
R.A.	07:41:18.81	09:21:28.32	07:21:08.81
Dec.	+31:14:34.2	+33:25:58.4	+34:48:08.7
Period [d]	1.30223	0.42647	0.404832
V [mag]	15.8	14.06	16.27
Spectral type	M3	M2	M3
RV [km s^{-1}]	121.5	4.8	–10.2
	Modeled parameter		
t_0 [MJD]	5849.469(1)	5322.1937(5)	4450.3046(3)
$(R_1+R_2)/a$	0.24(5)	0.53(7)	0.31(1)
R_2/R_1	1.58(2.99)	0.71(1.54)	1.16(7)
i [deg]	83.5(5.1)	73.5(9.7)	89.9(96.2)
e cos ω	–0.001(2)	0.001(3)	–0.005(1)
e sin ω	–0.1(1)	0.05(8)	–0.02(2)
K_1 [km s^{-1}]	89.8(9.3)	101.37†	124.89†
K_2 [km s^{-1}]	76.8(9.3)	141.63†	125.40†
$V_{\rm sys}$ [km s^{-1}]	119.5(6.7)	5.38†	–5.58†
	Derived parameter		
M_1 [$M_\odot$]	0.289	0.418	0.329
M_2 [$M_\odot$]	0.338	0.300	0.328
R_1 [$R_\odot$]	0.393	0.663	0.334
R_2 [$R_\odot$]	0.620	0.478	0.389
a [AU]	0.020	0.010	0.009

Notes: The errors are shown in parentheses (to the last digit).
† Unable to determine the error.

4 DISCUSSION

4.1 CSSJ074118.8+311434

The best-fit model from JKTEBOP indicates $M_1 = 0.289\,M_\odot$, $M_2 = 0.338\,M_\odot$, $R_1 = 0.393\,R_\odot$ and $R_2 = 0.62\,R_\odot$. Although the primary component is in good agreement with the empirical mass-radius relation of Demory et al. (2009), the secondary component's radius appears to be inflated. The inflated secondary stellar component might originate from a tidal locking effect exerted by the close companion, inducing enhanced stellar activity and inhibited convection, commonly seen in short period binaries (Kraus et al. 2011).

4.2 CSSJ092128.3+332558

The best-fit model from JKTEBOP indicates $M_1 = 0.716\,M_\odot$, $M_2 = 0.418\,M_\odot$, $R_1 = 0.299\,R_\odot$ and $R_2 = 0.663\,R_\odot$. Due to the limited observation time, we only obtained RV measurements at phase $\sim$0.25, hence JKTEBOP cannot provide reasonable error estimates of K_1, K_2 or $V_{\rm sys}$. Nevertheless, we note that the best-fit system velocity (5.38 km s^{-1}) is in good agreement with the system velocity from a single exposure by LAMOST (4.8 km s^{-1}), indicating our best-fit results are in the right

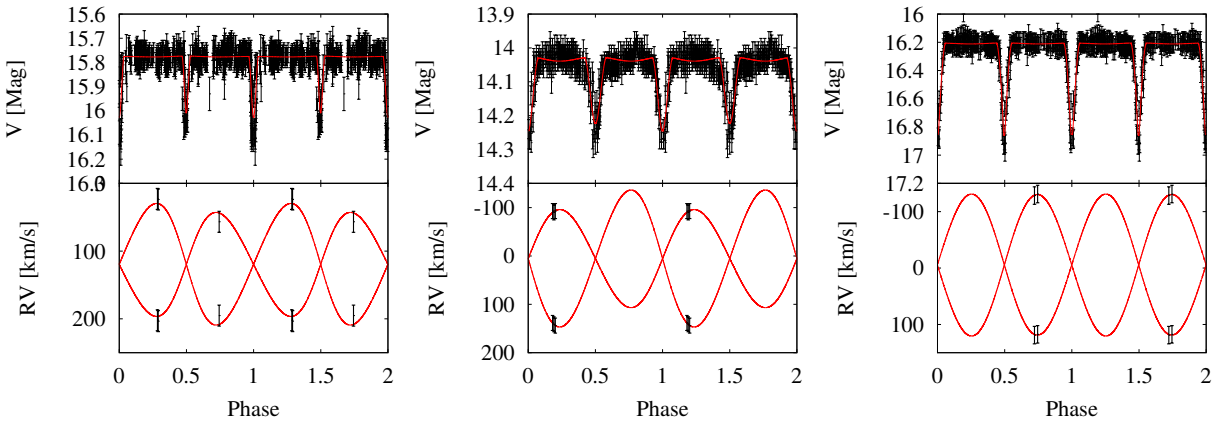

Fig. 2 Joint light curve and RV analysis of CSSJ074118.8+311434 (*left*), CSSJ092128.3+332558 (*middle*) and CSSJ072108.8 +344808 (*right*) using JKTEBOP.

ballpark. For CSSJ092128.3+332558, both stellar components show an enlarged radius compared to the mass radius relation of Demory et al. (2009), indicating both components are in tidal lock.

4.3 CSSJ072108.8+344808

The best-fit model from JKTEBOP indicates $M_1 = 0.329\,M_\odot$, $M_2 = 0.328\,M_\odot$, $R_1 = 0.334\,R_\odot$ and $R_2 = 0.389\,R_\odot$. Due to the limited observing time, we only obtained RVs at phase ∼0.75, so we were not able to obtain an error estimate from JKTEBOP. Nevertheless, we note that the best-fit system velocity (–5.58 km s^{-1}) is consistent with the system velocity from a single exposure (–10.2 km s^{-1}), indicating our best-fit results are in the right ballpark. For CSSJ072108.8+344808, both stellar components are in good agreement with the mass-radius relation of Demory et al. (2009).

5 SUMMARY AND PROSPECTS

We present a preliminary analysis of three double-lined M dwarf eclipsing binary systems discovered by cross-matching eclipsing binaries identified by the CSS and spectroscopic M dwarfs from LAMOST. We obtained follow-up, medium resolution spectra using GMOS on the Gemini North telescope, enabling us to disentangle the emission lines from both stellar components, and providing us with RV information during the RV maximum states. Our best-fit results suggest that both components of each eclipsing binary are composed of M dwarfs, and one of the stellar components of CSSJ074118.8+311434 even falls in the very low mass star regime ($M < 0.3\,M_\odot$), warranting further follow-ups. Due to the limited amount of available observation time, we were only able to obtain RV information at one quadrature for CSSJ092128.3+332558 and CSSJ072108.8+344808. Nevertheless, their best-fit systematic velocities are consistent with the RV from LAMOST single-shot spectra, indicating our best-fit parameters are in the right ballpark. Future high resolution spectroscopic observations will help pin down the uncertainties in fundamental parameters of these systems. Multi-epoch spectra, focusing on Hα or another indicator of stellar activity, will also shed light on the strength of stellar activity, as a means to test the tidal-locking induced inflation scenario.

Acknowledgements The Guo Shou Jing Telescope (the Large Sky Area Multi-Object Fiber Spectroscopic Telescope, LAMOST) is a National Major Scientific Project built by the Chinese Academy of Sciences. Funding for the project has been provided by the National Development and Reform Commission. LAMOST is operated and managed by National Astronomical Observatories, Chinese Academy of Sciences.

The CSS survey is funded by the National Aeronautics and Space Administration under Grant No. NNG05GF22G issued through the Science Mission Directorate Near-Earth Objects Observations Program. The CRTS survey is supported by the U.S.-National Science Foundation under grants AST-0909182.

Some of our results are based on observations obtained at the Gemini Observatory and processed using the Gemini IRAF package, which is operated by the Association of Universities for Research in Astronomy, Inc., under a cooperative agreement with the NSF on behalf of the Gemini partnership: the National Science Foundation (United States),

the National Research Council (Canada), CONICYT (Chile), Ministerio de Ciencia, Tecnología e Innovación Productiva (Argentina), and Ministério da Ciência, Tecnologia e Inovação (Brazil).

The authors wish to recognize and acknowledge the very significant cultural role and reverence that the summit of Mauna Kea has always had within the indigenous Hawaiian community. We are most fortunate to have the opportunity to conduct observations from this mountain.

References

Bertin, E., & Arnouts, S. 1996, A&AS, 117, 393
Covey, K. R., Ivezić, Ž., Schlegel, D., et al. 2007, AJ, 134, 2398
Cui, X.-Q., Zhao, Y.-H., Chu, Y.-Q., et al. 2012, RAA (Research in Astronomy and Astrophysics), 12, 1197
Demory, B.-O., Ségransan, D., Forveille, T., et al. 2009, A&A, 505, 205
Devor, J. 2005, ApJ, 628, 411
Drake, A. J., Djorgovski, S. G., Mahabal, A., et al. 2009, ApJ, 696, 870
Drake, A. J., Catelan, M., Djorgovski, S. G., et al. 2013, ApJ, 763, 32
Drake, A. J., Graham, M. J., Djorgovski, S. G., et al. 2014, ApJS, 213, 9
Dressing, C. D., & Charbonneau, D. 2013, ApJ, 767, 95
Guo, Y.-X., Yi, Z.-P., Luo, A.-L., et al. 2015, RAA (Research in Astronomy and Astrophysics), 15, 1182
Hook, I. M., Jørgensen, I., Allington-Smith, J. R., et al. 2004, PASP, 116, 425
Kraus, A. L., Tucker, R. A., Thompson, M. I., Craine, E. R., & Hillenbrand, L. A. 2011, ApJ, 728, 48
Lépine, S., & Gaidos, E. 2011, AJ, 142, 138
Nelder, J. A., & Mead, R. 1965, Computer Journal, 7, 308
Popper, D. M., & Etzel, P. B. 1981, AJ, 86, 102
Press, W. H., Teukolsky, S. A., Vetterling, W. T., & Flannery, B. P. 1992, Numerical Recipes in FORTRAN. The Art of Scientific Computing (Cambridge: Cambridge Univ. Press)
Seager, S., & Mallén-Ornelas, G. 2003, ApJ, 585, 1038
Southworth, J., Maxted, P. F. L., & Smalley, B. 2004, MNRAS, 351, 1277
Thompson, M. A., Kirkpatrick, J. D., Mace, G. N., et al. 2013, PASP, 125, 809
West, A. A., Morgan, D. P., Bochanski, J. J., et al. 2011, AJ, 141, 97
York, D. G., Adelman, J., Anderson, Jr., J. E., et al. 2000, AJ, 120, 1579
Zhou, G., Bayliss, D., Hartman, J. D., et al. 2015, MNRAS, 451, 2263